

Pressure-Induced Polymerization and Disproportionation of Li_2C_2 Accompanied with Irreversible Conductivity Enhancement

Lijuan Wang,^{†,◆} Xiao Dong,^{†,◆} Yajie Wang,[†] Haiyan Zheng,^{*,†,ID} Kuo Li,^{*,†} Xing Peng,[‡] Ho-kwang Mao,^{†,§,||} Changqing Jin,^{*,⊥,#} Yufei Meng,[†] Mingquan Huang,[▽] and Zhisheng Zhao[○]

[†]Center for High Pressure Science and Technology Advanced Research, Beijing, 100094, People's Republic of China

[‡]Thermo Fisher Scientific Company, Xinqiniao Road No. 27, Building 6, Pudong, Shanghai, 201206, People's Republic of China

[§]HPSynC, Geophysical Laboratory, Carnegie Institution of Washington, Argonne, Illinois 60439, United States

^{||}Geophysical Laboratory, Carnegie Institution of Washington, Washington, District of Columbia 20015, United States

[⊥]Institute of Physics, Chinese Academy of Science, Beijing, 100190, People's Republic of China

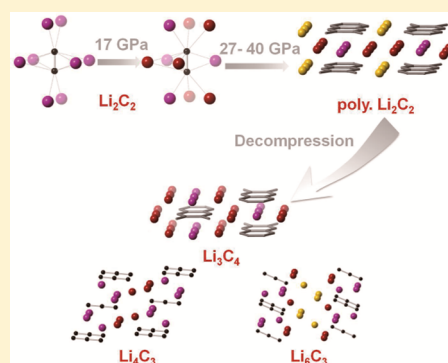
[#]Collaborative Innovation Centre of Quantum Matter, Beijing, 100871, People's Republic of China

[▽]Beijing Key Laboratory of Flavor Chemistry, Beijing Technology and Business University, Beijing, 100048, China

[○]State Key Laboratory of Metastable Materials Science and Technology, Yanshan University, Qinhuangdao, 066004, China

Supporting Information

ABSTRACT: Li_2C_2 has the highest theoretical capacity ($1400 \text{ mA}\cdot\text{h}\cdot\text{g}^{-1}$) as the electrode material for Li-ion battery, but suffers from low conductivity. Here we found that under external pressure its conductivity was irreversibly enhanced by 10^9 -fold. To explain that, we performed X-ray diffraction, Raman, IR, gas chromatography–mass spectrometry, and theoretical investigations under external pressure. We found that the C_2^{2-} anions approached to each other and polymerized upon compression, which is responsible for the irreversible enhancement of conductivity. The polymer has a ribbon structure and disproportionates into Li_3C_4 ($\text{Li}_{2-0.5}\text{C}_2$) ribbon structure, Li_6C_3 (Li propenide) and Li_4C_3 (Li allenide) upon decompression, implying that the carbon skeletal is highly electrochemically active. Our work reported polymerized Li_2C_2 for the first time, demonstrated that applying pressure is an effective method to prepare novel Li–C frameworks, and hence shed light on the search for novel carbon-based electrode materials.



Li–C compounds have been widely investigated due to their applications in Li-ion battery materials. For example, Li-intercalated graphite is used in the anode of a rechargeable Li-ion battery, because it is conductive and can avoid Li dendrites.¹ Recently, a very simple Li salt, lithium acetylide (Li_2C_2), was reported to be electrochemically active, through an oxidation-dimerization process from 2C_2^{2-} to C_4 .² As a cathode material, half of the lithium can be extracted, which corresponds to a capacity of $700 \text{ mAh}\cdot\text{g}^{-1}$. However, the C_2^{2-} anions are isolated from each other, hindering the electron transfer, and the conductivity is too low for application.

High pressure provides a straightforward method to build up conductive conjugated double-bond backbones, through addition polymerization of triple-bond monomers. This is also referred as pressure-induced polymerization (PIP), and was reported for many molecular compounds like acetylene,^{3–5} ethylene,^{6–8} and hydrogen cyanide^{9,10} as well as ionic compounds like metal cyanide^{11–14} and acetylide.^{15–17} Under high pressure, a rich diversity of carbon structures in Li–C compounds including the nanoribbon, sheets, and frameworks were predicted, most of which are metallic.¹⁸ Li_2C_2 was also

predicted to polymerize to form Li polyacetylide and Li graphenide under external pressure,^{19,20} and its phase transitions were investigated experimentally.²¹ However, up to now, there is no any experimental evidence for the polymers. In this work, we investigated the structural transitions and the corresponding conductivity of Li_2C_2 experimentally under high pressure. We found that the acetylide anions in Li_2C_2 polymerized under compression, and the electrical conductivity was enhanced by 10^9 -fold and recoverable to ambient pressure, which suggests that the polymerized Li_2C_2 has a potential application in Li-battery materials.

Figure 1 presents the resistivity of Li_2C_2 under external pressure. At ambient pressure, Li_2C_2 had a resistivity of $10^6 \text{ Ohm}\cdot\text{m}$, and decreased upon compression. The resistivity dropped by ~ 3 orders of magnitude around 17–20 GPa, and had a discontinuity at 28 GPa, indicating two phase transitions. When compressed to above 45 GPa, the resistivity decreased by

Received: July 11, 2017

Accepted: August 18, 2017

Published: August 18, 2017

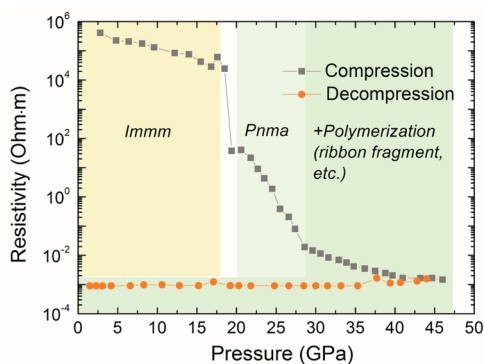


Figure 1. Resistivity of Li_2C_2 under external pressure.

9 orders of magnitude compared to that at ambient pressure. When decompressed, the resistivity almost remained constant at 10^{-3} Ohm·m, which suggests that an irreversible bonding process occurred above 35–40 GPa.

To understand the structural evolution under external pressure, in situ synchrotron X-ray diffraction (XRD) was measured (Figure S1). At ambient pressure, Li_2C_2 crystallized in the orthorhombic structure (space group $Immm$).²¹ When compressed to 17.1 GPa, a new phase appeared and was indexed with an orthorhombic lattice ($Pnma$).²¹ Above 28.6 GPa, a few new peaks were observed (marked by the dots in Figure S1), indicating another phase transition. These two transitions were recognized as the reason for the two discontinuities observed in the resistivity curve (Figure 1).

To explore the variation of the functional groups, in situ Raman spectra were measured (Figure S2). Similar to previously reported results,^{21,22} an additional peak attributed to the $\text{C}\equiv\text{C}$ stretching mode appeared at around 16 GPa, which corresponded to the $Pnma$ phase (Figure S2b). At pressures above 29 GPa, the Raman spectra became featureless up to 40 GPa and upon decompression. However, when the pressure was released to zero in the air, a peak corresponding to the $\text{C}=\text{C}$ stretching mode appeared around 1600 cm^{-1} (Figure S3). This is because the polymeric carbide anions only showed strong Raman signal after absorbing moisture and forming hydrocarbons, and therefore evidenced the PIP of C_2^{2-} . A similar Raman mode was also observed in recovered CaC_2 and used to evidence the irreversible polymerization of C_2^{2-} , but at a lower pressure (>25 GPa for CaC_2 vs >35 GPa for Li_2C_2).¹⁷ It is worthy to note that only the Li_2C_2 recovered from pressures above 35 GPa showed this $\text{C}=\text{C}$ stretching mode (and hence irreversible polymerization, Figure S3), which should be responsible for the recoverable high conductivity phase observed at pressures above 35 GPa. It also suggests another process proceeded above 35 GPa.

In situ IR absorptions provided more information (Figure 2a). Above 18 GPa (in $Pnma$ phase), several weak bands grew around 700 cm^{-1} and between 800 and 1000 cm^{-1} . Above ~ 27 GPa, the band around 700 cm^{-1} disappeared, and three peaks were observed in the range of 1100 – 1300 cm^{-1} , which gradually disappeared above ~ 35 GPa, and remained silent upon downloading. Above 35 GPa, the sample also became highly absorbent, much stronger than those under lower pressure, and probably metallic. When decompressed below 14 GPa, several bands gradually grew at 700 – 800 cm^{-1} and 1600 – 1700 cm^{-1} . Meanwhile, the bands at 800 – 1000 cm^{-1} also disappeared below 10 GPa. The transitions (~ 18 , 27, and 35 GPa upon compression) were in good agreement with the

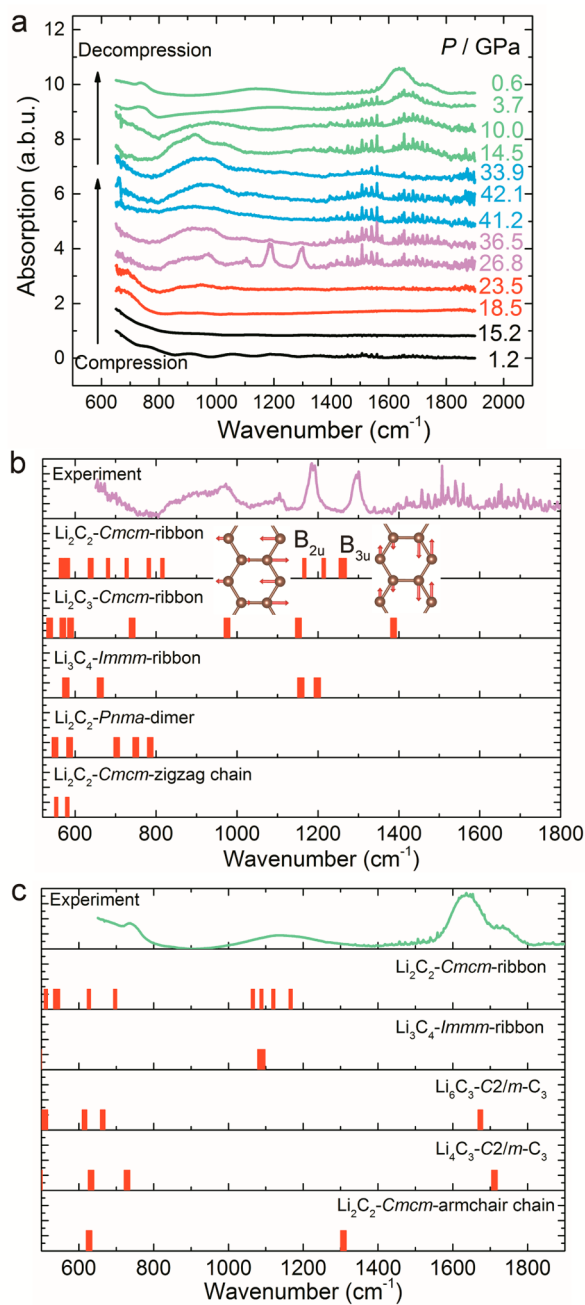
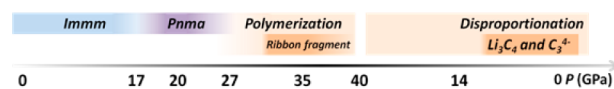


Figure 2. IR spectra of the Li_2C_2 (experiment) and the predicted Li–C phases (simulation) under external pressure. (a) Selected experimental data. Theoretical simulations of selected phases at (b) 27 GPa and (c) 1 GPa (recovered).

phase transitions detected by Raman, XRD, and resistivity experiments, and are summarized in Scheme 1. As discussed below, Li_2C_2 transformed from $Immm$ to $Pnma$ phase when compressed up to 17 GPa, polymerized above 27 GPa, and generated some unknown irreversible products at ~ 35 GPa.

Scheme 1. Phase Relations of Li_2C_2 under External Pressure



To recognize the phases under high pressure, we calculated the IR spectra of all the predicted phases in this pressure range (Figure 2, Figures S4 and S5).^{18–20} At 1 GPa, the Li_2C_2 *Immm* phase had no infrared active mode above 500 cm^{-1} (Figure S5). When it transformed to the *Pnma* phase, the Li–C interaction was strengthened (Figure 2b Li_2C_2 -*Pnma*-dimer), resulting in the half hump at 700 cm^{-1} (Figure 2a, 18.5 GPa). As shown in Figure 2b, after careful comparison, the new peaks observed at 1187 and 1296 cm^{-1} above 27 GPa are recognized as the in-plane transverse mode and longitudinal mode of the charged carbon ribbons in lithium polyacene. This is significant evidence supporting the PIP of C_2^{2-} at 27 GPa. Among the predicted Li–C structures, three phases have polyacene substructure, Li_2C_2 -*Cmcm*-ribbon (note that there is another Li_2C_2 -*Cmcm*-zigzag phase with zigzag carbon chains),²⁰ Li_2C_3 -*Cmcm*, and Li_3C_4 -*Immm*.^{18,20} At 27 GPa, the peak positions of the Li_2C_2 -*Cmcm*-ribbon were calculated to be 1166 and 1266 cm^{-1} , close to those observed in experiment, while for Li_2C_3 -*Cmcm* they were 1151 and 1386 cm^{-1} and for Li_3C_4 -*Immm* were 1157 and 1198 cm^{-1} , respectively. In addition, the difference between these two peaks was 109 cm^{-1} , which is similar to the Li_2C_2 -*Cmcm*-ribbon (100 cm^{-1}), but in Li_2C_3 -*Cmcm* and Li_3C_4 -*Immm*, they were 235 and 41 cm^{-1} , respectively. Therefore, we attribute the peaks observed experimentally to the fragment of the Li_2C_2 -*Cmcm*-ribbon phase; the vibration modes are shown in the inset of Figure 2.

For the downloading process, the peaks at 1636 and 1733 cm^{-1} (0.6 GPa) were identified as the C–C stretching vibration of the C_3 anions (Figure 2c and Figure S5). In all thermodynamically stable Li–C phases, only Li propenide Li_6C_3 -*C2/m* and Li allenide Li_4C_3 -*C2/m* contain C_3 anions, with infrared absorptions at 1673 and 1711 cm^{-1} at 1 GPa, respectively, which fit the experimental data very well (Figure 2c and Figure S5). Therefore, these two peaks imply the coexistence of amorphous Li_6C_3 and Li_4C_3 . For the broad band around 1100 cm^{-1} , considering the balance in the stoichiometric ratio of Li:C = 1:1, we attribute it to the merged peaks of the in-plane transverse mode and longitudinal mode of the charged carbon ribbons in the Li_3C_4 -*Immm* fragments (1087 and 1089 cm^{-1} at 1 GPa). However, the Li_2C_2 -*Cmcm*-ribbon cannot be excluded because its featured peaks (1065 , 1088 , 1120 , and 1166 cm^{-1} at 1 GPa) are also in this region. Thus, the IR spectra upon decompression uncovered two kinds of C_3 anions and one (or more) ribbon component, most reasonably explained by noncrystallized Li_6C_3 -*C2/m*, Li_4C_3 -*C2/m*, and Li_3C_4 -*Immm* phases, which indicates a disproportionation decomposition of Li_2C_2 .

So far, the phase transitions and chemical transitions are well understood. The Li_2C_2 -*Immm*-dimer transformed to a Li_2C_2 -*Pnma*-dimer above 16 GPa due to restacking of Li^+ and C_2^{2-} upon compression. Above $\sim 27\text{ GPa}$, Li_2C_2 started to polymerize into a Li_2C_2 ribbon structure. This structure is not thermodynamically stable according to theoretical predictions and did not crystallize under experimental conditions, whereas Li_3C_4 , with the same ribbon structure but less lithium, is stable.¹⁸ Hence, Li_2C_2 tends to disproportionate into a C-rich phase (Li_3C_4) and Li-rich phases (Li_4C_3 , etc.). When decompressed, the disproportionation is accelerated, and the signals from fragments like C_3^{4-} are more pronounced. For the conductivity, the compression of the distances between C_2^{2-} should be the main reason for the enhancement of the conductivity, and the PIP of C_2^{2-} is responsible for the irreversibility.

More solid evidence supporting the PIP is given by gas chromatography–mass spectrometry (GC–MS) analysis. We identified tens of hydrocarbons that contain six or more carbon atoms in the deconvoluted spectra of the hydrolyzed products of the recovered samples, like C_6H_8 and C_8H_{10} . Selected hydrocarbons are listed in Table S1. The relative peak area and the corresponding retention time of the hydrocarbons, as well as their stoichiometry, are summarized in Figure 3. These

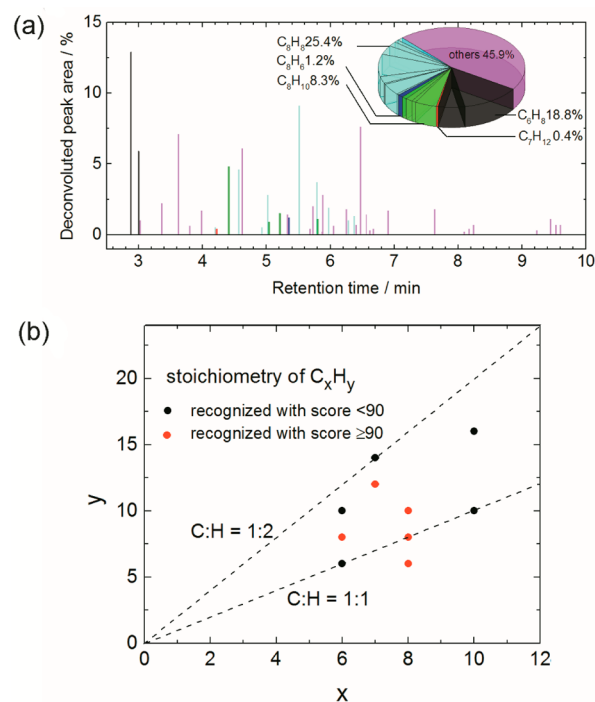


Figure 3. (a) Relative area of the deconvoluted peaks of the hydrocarbons in the hydrolyzed product. The black, red, green, blue, and cyan slices and bars are for components separated by GC and identified by MS with the C_6H_8 , C_7H_{12} , C_8H_{10} , C_8H_6 , and C_3H_8 formulas, including several isomers in each, respectively. The components with a score lower than 90 are counted in “others”. (b) Stoichiometry of the hydrocarbons. Scores lower than 90 only suggest the product assignment is not very satisfactory, while the m/z values of the molecular ions still have good accuracies.

molecules were absent in the hydrolyzed product of the raw material and thus demonstrated the PIP of C_2^{2-} . Almost all of the suggested structures (score ≥ 90) have ring structures (like styrene, ethylbenzene, etc.). This indicates that the ring structure is popular in the carbon skeleton and thus supports the ribbon structures in the PIP product. Most of the recognized components still had stoichiometry around C:H = 1:1 (Figure 3b), which agrees with the oxidation state of Li_2C_2 , and suggests addition polymerizations of C_2^{2-} . However, products with a C:H ratio significantly deviating from 1:1 were also observed (like C_7H_{12} , Figure 3b), suggesting that some carbon atoms were oxidized or reduced, and a disproportionation reaction occurred, in agreement with our IR experiments. This disproportionation also demonstrates the electrochemical activity of the Li polyacene, which is potentially useful when designing an electrode material.

Such a disproportionation was not observed in the PIP of CaC_2 .¹⁷ This is probably because Li^+ is monovalent and can flexibly compensate the charges of carbon skeleton. Li^+ is also more active in diffusion to accelerate the disproportionation

and the following phase separation. By contrast, Ca^{2+} is divalent and less diffusive, and high temperature is likely needed to obtain the thermodynamically stable phase.

In conclusion, we found a 10^9 -fold enhancement of conductivity of Li_2C_2 under external pressures up to and above 40 GPa, and uncovered the reason by investigating the phase transitions and chemical reactions. Li_2C_2 polymerizes into a Li_2C_2 -*Cmcm*-ribbon during compression, and then decomposes into two C_3 phases and one ribbon phase, most likely noncrystallized Li_6C_3 , Li_4C_3 , and Li_3C_4 during decompression. The polymerization and the following disproportionation reaction are evidenced by GC-MS analysis of the recovered sample. This investigation synthesized the Li polycarbide for the first time, provides a detailed scheme of the whole reaction process, and suggests that applying pressure is a promising method to modify the carbon skeleton and improve the conductivity of Li-C compounds. The highly conductive compressed Li_2C_2 can be recovered to ambient pressure, indicating it may have potential applications in Li-ion battery.

■ ASSOCIATED CONTENT

📄 Supporting Information

The Supporting Information is available free of charge on the ACS Publications website at DOI: 10.1021/acs.jpclett.7b01779.

Details about the synthesis of Li_2C_2 and Li_2C_2 recovered from high pressure for the GC-MS measurement; in situ XRD, Raman, IR and impedance experiments; first principle calculations on the structural relaxation and spectrum properties; GC-MS measurements; selected XRD and Raman patterns of Li_2C_2 under high pressure (Figure S1 and S2); Raman spectra of the sample recovered from high pressure (Figure S3); calculated IR spectra (27 and 1 GPa) of all the phases predicted to be stable from 0 to 40 GPa (Figure S4 and S5); selected high-resolution mass spectrum results of Li_2C_2 recovered from high pressure (Table S1) (PDF)

■ AUTHOR INFORMATION

Corresponding Authors

*E-mail: zhenghy@hpstar.ac.cn.

*E-mail: likuo@hpstar.ac.cn.

*E-mail: Jin@iphy.ac.cn.

ORCID

Haiyan Zheng: 0000-0002-4727-5912

Author Contributions

◆ These authors contributed equally.

Notes

The authors declare no competing financial interest.

■ ACKNOWLEDGMENTS

The authors acknowledge the support of the NSAF (Grant No.: U1530402) and the National Natural Science Foundation of China (NSFC) (Grant Nos.: 21501162, 21601007 and 21771011). A portion of this research was performed at HPCAT (Sector 16), Advanced Photon Source (APS), Argonne National Laboratory. HPCAT (Geophysical Lab) operations are supported by DOENNSA under Award No. DE-NA0001974 and DOE-BES under Award No. DE-FG02-99ER45775, with partial instrumentation funding by NSF. APS is supported by DOE-BES, under Contract No. DE-AC02-

06CH11357. The authors thank Dr. Yue Meng for supporting the in situ X-ray diffraction measurements under high pressure. The authors also thank the Thermo Fisher Scientific company for their assistance with the GC-MS measurement. The calculation was performed on the TianheII supercomputer at Chinese National Supercomputer Center in Guangzhou.

■ REFERENCES

- (1) Chevallier, F.; Poli, F.; Montigny, B.; Letellier, M. In Situ ^7Li Nuclear Magnetic Resonance Observation of the Electrochemical Intercalation of Lithium in Graphite: Second Cycle Analysis. *Carbon* **2013**, *61*, 140–153.
- (2) Tian, N.; Gao, Y.; Li, Y.; Wang, Z.; Song, X.; Chen, L. Li_2C_2 , a High-capacity Cathode Material for Lithium Ion Batteries. *Angew. Chem.* **2016**, *128*, 654–658; *Angew. Chem., Int. Ed.* **2016**, *55*, 644–648.
- (3) Aoki, K.; Usuba, S.; Yoshida, M.; Kakudate, Y.; Tanaka, K.; Fujiwara, S. Raman Study of the Solid-state Polymerization of Acetylene at High Pressure. *J. Chem. Phys.* **1988**, *89*, 529–534.
- (4) Ceppatelli, M.; Santoro, M.; Bini, R.; Schettino, V. Fourier Transform Infrared Study of the Pressure and Laser Induced Polymerization of Solid Acetylene. *J. Chem. Phys.* **2000**, *113*, 5991–6000.
- (5) Trout, C. C.; Badding, J. V. Solid State Polymerization of Acetylene at High Pressure and Low Temperature. *J. Phys. Chem. A* **2000**, *104*, 8142–8145.
- (6) Chelazzi, D.; Ceppatelli, M.; Santoro, M.; Bini, R.; Schettino, V. High-pressure Synthesis of Crystalline Polyethylene using Optical Catalysis. *Nat. Mater.* **2004**, *3*, 470–475.
- (7) Citroni, M.; Ceppatelli, M.; Bini, R.; Schettino, V. Laser-induced Selectivity for Dimerization versus Polymerization of Butadiene under Pressure. *Science* **2002**, *295*, 2058–2060.
- (8) Chelazzi, D.; Ceppatelli, M.; Santoro, M.; Bini, R.; Schettino, V. Pressure-induced Polymerization in Solid Ethylene. *J. Phys. Chem. B* **2005**, *109*, 21658–21663.
- (9) Khazaei, M.; Liang, Y.; Bahramy, M. S.; Pichierri, F.; Esfarjani, K.; Kawazoe, Y. High-pressure Phases of Hydrogen Cyanide: Formation of Hydrogenated Carbon Nitride Polymers and Layers and Their Electronic Properties. *J. Phys.: Condens. Matter* **2011**, *23*, 405403.
- (10) Aoki, K.; Baer, B. J.; Cynn, H. C.; Nicol, M. High-pressure Raman Study of One-Dimensional Crystals of the Very Polar Molecule Hydrogen Cyanide. *Phys. Rev. B: Condens. Matter Mater. Phys.* **1990**, *42*, 4298–4303.
- (11) Chen, J.-Y.; Yoo, C.-S. Physical and Chemical Transformations of Sodium Cyanide at High Pressures. *J. Chem. Phys.* **2009**, *131*, 144507.
- (12) Li, K.; Zheng, H.; Hattori, T.; Sano-Furukawa, A.; Tulk, C. A.; Molaison, J.; Feyngenson, M.; Ivanov, I. N.; Yang, W.; Mao, H.-k. Synthesis, Structure, and Pressure-induced Polymerization of $\text{Li}_3\text{Fe}(\text{CN})_6$ Accompanied with Enhanced Conductivity. *Inorg. Chem.* **2015**, *54*, 11276–11282.
- (13) Li, K.; Zheng, H.; Wang, L.; Tulk, C. A.; Molaison, J. J.; Feyngenson, M.; Yang, W.; Guthrie, M.; Mao, H.-k. $\text{K}_3\text{Fe}(\text{CN})_6$ under External Pressure: Dimerization of CN^- Coupled with Electron Transfer to Fe(III). *J. Phys. Chem. C* **2015**, *119*, 22351–22356.
- (14) Li, K.; Zheng, H.; Ivanov, I. N.; Guthrie, M.; Xiao, Y.; Yang, W.; Tulk, C. A.; Zhao, Y.; Mao, H.-k. $\text{K}_3\text{Fe}(\text{CN})_6$: Pressure-induced Polymerization and Enhanced Conductivity. *J. Phys. Chem. C* **2013**, *117*, 24174–24180.
- (15) Li, Y.-L.; Luo, W.; Zeng, Z.; Lin, H.-Q.; Mao, H.-k.; Ahuja, R. Pressure-induced Superconductivity in CaC_2 . *Proc. Natl. Acad. Sci. U. S. A.* **2013**, *110*, 9289–9294.
- (16) Li, Y.-L.; Wang, S.-N.; Oganov, A. R.; Gou, H.; Smith, J. S.; Strobel, T. A. Investigation of Exotic Stable Calcium Carbides Using Theory and Experiment. *Nat. Commun.* **2015**, *6*, 6974.
- (17) Zheng, H.; Wang, L.; Li, K.; Yang, Y.; Wang, Y.; Wu, J.; Dong, X.; Wang, C.-H.; Tulk, C. A.; Molaison, J. J.; Ivanov, I. N.; Feyngenson, M.; Yang, W.; Guthrie, M.; Zhao, Y.; Mao, H.-k.; Jin, C. Pressure

Induced Polymerization of Acetylide Anions in CaC_2 and 10^7 Fold Enhancement of Electrical Conductivity. *Chem. Sci.* **2017**, *8*, 298–304.

(18) Lin, Y.; Strobel, T. A.; Cohen, R. E. Structural Diversity in Lithium Carbides. *Phys. Rev. B: Condens. Matter Mater. Phys.* **2015**, *92*, 214106.

(19) Chen, X.-Q.; Fu, C. L.; Franchini, C. Polymeric Forms of Carbon in Dense Lithium Carbide. *J. Phys.: Condens. Matter* **2010**, *22*, 292201.

(20) Benson, D.; Li, Y.; Luo, W.; Ahuja, R.; Svensson, G.; Häussermann, U. Lithium and Calcium Carbides with Polymeric Carbon Structures. *Inorg. Chem.* **2013**, *52*, 6402–6406.

(21) Efthimiopoulos, I.; Benson, D. E.; Konar, S.; Nylén, J.; Svensson, G.; Häussermann, U.; Liebig, S.; Ruschewitz, U.; Vazhenin, G. V.; Loa, I.; Hanfland, M.; Syassen, K. Structural Transformations of Li_2C_2 at High Pressures. *Phys. Rev. B: Condens. Matter Mater. Phys.* **2015**, *92*, 064111.

(22) Nylén, J.; Konar, S.; Lazor, P.; Benson, D.; Häussermann, U. Structural Behavior of the Acetylide Carbides Li_2C_2 and CaC_2 at High Pressure. *J. Chem. Phys.* **2012**, *137*, 224507.